Molecular Structure of 3,4-Difluorofuran-2,5-dione (Difluoromaleic Anhydride) As Determined by Electron Diffraction and Microwave Spectroscopy in the Gas Phase and by Theoretical Computations

Basil T. Abdo,[†] Halima Amer,[‡] R. Eric Banks,[†] Paul T. Brain,[‡] A. Peter Cox,[§] Oliver J. Dunning,[§] Vincent Murtagh,[†] David W. H. Rankin,*[,‡] Heather E. Robertson,[‡] and Bruce A. Smart[‡]

Department of Chemistry, U.M.I.S.T., P.O. Box 88, Manchester, M60 1QD, U.K., Department of Chemistry, University of Edinburgh, West Mains Road, Edinburgh, EH9 3JJ, U.K., and School of Chemistry, The University, Cantock's Close, Bristol, BS8 1TS, U.K.

Received: November 30, 1998; In Final Form: January 15, 1999

The structure of 3,4-difluorofuran-2,5-dione has been determined experimentally in the gas phase by microwave spectroscopy using rotation constants derived from five isotopomers and by a combined analysis of electron-diffraction and microwave data. The geometry is planar with C_{2v} symmetry. Structural parameters [distances ($r_\alpha°$)/pm, angles $\angle_\alpha$/deg, (1σ errors)] for the combined analysis are: r(C═O) = 119.0(1); r(C−F) = 130.9(2); r(C═C) = 133.2(3); r(O−C) = 139.3(1); r(C−C) = 148.5(2); ∠C−C═C = 108.3(1); ∠C═C−F = 129.9-(1); ∠C−C═O = 129.3(1); ∠C−O−C = 108.9(1); ∠O−C−C = 107.2(1). These values are in excellent agreement with those obtained in an ab initio study of the molecular geometry at the MP2/6-311+G*(2df) level of theory. The dipole moment of difluoromaleic anhydride has been determined experimentally by Stark-effect measurements to be 1.867(3) D.

Introduction

Saturation of the C═C double bond in 3,4-difluorofuran-2,5-dione (difluoromaleic anhydride) (**1**) with bis(trifluoromethyl)-amino-oxyl, $(CF_3)_2NO$, occurs smoothly at 60 °C during 24 h to give the corresponding 1:2 adduct virtually quantitatively.[1] This adduct is under investigation as a precursor (via reactions involving the anhydride function) of surfactants suitable, for example, as a means of preparing emulsions from "blood substitutes" (oxygen carriers), synthesized via saturation of C═C bonds in perfluoro-alkanes and -cycloalkanes with $(CF_3)_2$-NO.[1,2] The need to prepare difluoromaleic anhydride for this project enabled a structural investigation of this potentially important compound to be carried out.

Although all four dihalomaleic anhydrides are known[3−6] (dichloromaleic anhydride having been first reported in 1883[4]), it has been the parent compound, maleic anhydride itself, that has received greatest attention, in terms of both its physical properties and characterization, including a study of its gas-phase structure by electron diffraction (GED)[7] and microwave (MW) spectroscopy,[8] and its chemical reactivity.[9] Of the dihalo derivatives, structural parameters are available only for dichloromaleic anhydride as refined from its electron-diffraction pattern.[10] Considering the difference in size and electronegativity between chlorine and hydrogen,[11] it was surprising to discover from the gas-phase studies that there is very little difference between the structures of the parent and its dichloro derivative.[7,10] To investigate this further, and as part of a wider study of small fluorocarbons and fluorinated organometallic compounds,[12,13] we have determined the structure of difluoromaleic anhydride in the gas phase by microwave spectroscopy and electron diffraction. In addition, theoretical computations for maleic anhydride and its dihalo derivatives (X = F, Cl, and Br) are reported in support of our experimental conclusions.

Experimental Section

Preparation of Difluoromaleic Anhydride (1). Although shorter routes are known, e.g., the oxidation of commercially available pentafluorophenol with peracetic acid,[14] followed by dehydration of the difluoromaleic acid thus formed, the classical multi-stage DuPont route[3] outlined in Scheme 1 was chosen. This approach provides trifluorosuccinic acid (**3**) and also can be modified to give 2,2-difluorosuccinic acid and monofluoromaleic anhydride, all products needed for associated studies involving $(CF_3)_2NO$.

The key intermediate in the DuPont synthetic scheme is 1,1,2-trichloro-2,3,3-trifluorocyclobutane (**4**), prepared by a thermal [2 + 2] cycloaddition reaction between the commercial olefins chlorotrifluoroethene (bp −28.5 °C; Fluorochem, U.K.) and 1,1-dichloroethene (bp 30−32 °C; Aldrich). Only this first stage requires special equipment (a 1-liter stainless steel Magnedrive autoclave was used, providing ca. 300 g of analytically pure redistilled **4** per run) and techniques (high pressure and gas handling). Extensive polymer formation (despite the use of hydroquinone as an inhibitor)[3] is responsible for the moderate yield of **4** (lit.[3] 48%; this work, 52%) and also creates autoclave-cleaning problems, not mentioned previously.[3] The polymeric material formed in our work tended to adhere strongly to the inner wall of the autoclave; it was easily removed by pouring hot water into the cup, the differential expansion (steel vs polymer) causing the organic material to peel off, leaving a clean metal surface. (**Note**: This cleaning operation must be carried out in an efficient fume cupboard so that any volatile organic material released is not inhaled by the operator.)

* Author to whom correspondence should be addressed.
[†] Department of chemistry, U.M.I.S.T.
[‡] Department of Chemistry, University of Edinburgh.
[§] School of Chemistry, The University.

10.1021/jp984554o CCC: $18.00 © 1999 American Chemical Society
Published on Web 03/05/1999

SCHEME 1

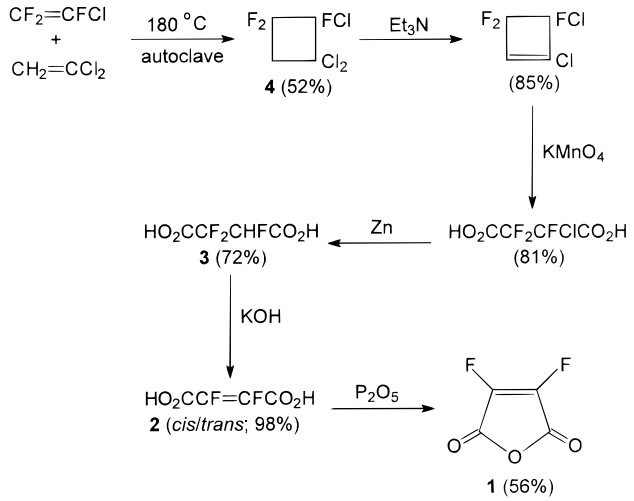

In the present work, only the yield reported for the final step in Scheme 1 (89% of **1**)[3] was not matched. The best yield of **1** was achieved by heating an intimate mixture of phosphorus pentoxide (14.2 g, 100 mmol) with the mixed difluoromaleic and difluorofumaric acids (**2**) (15.0 g, 98 mmol) at 70 °C (oil-bath temperature) in vacuo in the stillpot (100 cm^3; equipped with a PTFE-coated stirrer bar) of a Vigreux distillation unit. The crude difluoromaleic anhydride was collected, as it formed, in a cooled (ice) receiver and redistilled to give 7.3 g (54.5 mmol, 56%) of a clear, colorless, viscous liquid (bp 127−129 °C; lit.[3] 128 °C) which was identified as difluoromaleic anhydride (**1**) by ^{13}C and ^{19}F NMR spectroscopy [δ_C 138.2 (d, $^1J_{CF}$ 302 Hz), 155.3 (m) ppm; δ_F −61.5 (s) ppm (CF_3CO_2H ref)].

For microwave spectroscopy (see below), samples were enriched with ^{18}O on a millimolar scale by hydrolysis of difluoromaleic anhydride with excess water enriched 40% in ^{18}O. After equilibration, the mixture was distilled to remove the excess water from the maleic acid product. The acid was then mixed with P_2O_5 and the enriched maleic anhydride sublimed from the mixture by gentle heating in vacuo. The proportion $H_2{}^{18}O/H_2{}^{16}O$ taken optimized the yield of the single-substituted ^{18}O isotopomers in order to simplify measurement of the spectra.

Electron Diffraction. Electron scattering intensities were recorded on Kodak Electron Image plates using the Edinburgh gas diffraction apparatus.[15] The sample and nozzle were maintained at ca. 293 K during the exposure of three and two plates, respectively, at the long (286 mm) and short (128 mm) camera distances. Scattering intensities for benzene were also recorded, to provide calibration of the camera distances and the electron wavelength. The plates were traced using a computer-controlled Joyce Loebl MDM6 microdensitometer at the EPSRC Daresbury Laboratory.[16] Analysis of the data made use of standard data reduction[16] and least-squares refinement[17] programs and scattering factors.[18] The *s* ranges, weighting points, and other experimental details are listed in Table 1.

Rotational Spectroscopy. Microwave spectra were measured using a conventional Stark modulation spectrometer operating at 100 kHz. Gas samples at 3−10 Pa were introduced into a 3-m stainless steel X-band absorption cell, cooled to ca. 243 K. Under these conditions the sample was stable, no degradation in the spectrum being visible after ca. 8 h. For assignment purposes, low-resolution spectra were taken using backward-wave oscillator sources in the 8−40 GHz region. Assignment was initially made by measurement of strong, high *J* transitions ($J = 18-27$) thrown down by asymmetry into the 8−12 GHz region. The two singly substituted ^{18}O species were measured using Stark spectroscopy on enriched samples. The assignment of the exo-substituted species was confirmed by radio frequency-microwave double resonance using the small μ_a component of the dipole generated by the rotation of the principal axes. This method was not available for the C_{2v} species since it possesses only a μ_b component of the dipole. Carbon-13 lines were measured in natural abundance at Exeter University in collaboration with Professor A. C. Legon using Fourier transform microwave spectroscopy on the sample in free jet expansion. Transition frequencies and their assignments for the five isotopomers are given in Table 2 and the spectroscopic constants in Table 3.

Vibrational and NMR Spectroscopy. Infrared spectra in the range 4000−400 cm^{-1} were recorded using a Mattson "Galaxy" FT spectrometer employing a standard 10-cm gas cell equipped with CsI windows. For Raman spectroscopy, the sample was presented as a liquid at room temperature sealed in an evacuated, Pyrex-glass ampule. Spectra were recorded in the range 2000−50 cm^{-1} using a Dilor "LabRam" Raman microscope. The observed frequencies are reported in the Supporting Information. NMR spectra were recorded at room temperature for a solution in $CFCl_3$ on Bruker AC-300 (^{13}C, 75.5 MHz, external TMS reference) and AC-200 (^{19}F, 188.8 MHz, external CF_3CO_2H reference) spectrometers.

Ab Initio Calculations. All ab initio molecular orbital calculations were carried out on a DEC Alpha APX 1000 workstation using the Gaussian 94 program.[19] Geometry optimizations on difluoromaleic anhydride were undertaken at the SCF and MP2 levels using the standard 6-31G(d)[20−22] and 6-311G(d)[23,24] basis sets. To investigate the effects of diffuse functions and larger polarization sets, geometry optimizations were undertaken also at the MP2 level using the 6-311G(2df) and 6-311+G(2df) basis sets (Table 4). Harmonic force-field calculations were undertaken at the SCF/6-31G(d) and MP2/6-31G(d) levels; fundamental frequencies from the latter are listed in Table 5. Subsequently, frequency calculations using the larger 6-311G(d) basis set were performed at the MP2 and B3LYP levels to verify the ordering of the lowest two modes.

Force-Field Calculations. The program ASYM40[25] was used to convert the theoretical (MP2/6-31G(d) level) Cartesian force field to one described by symmetry coordinates. An optimum fit of the theoretical to the experimental frequencies was achieved by a refinement of the ab initio force constants using eight scaling factors. Details, including a list of the internal and symmetry coordinates, are given as part of the Supporting Information. Root-mean-square amplitudes of vibration (*u*), perpendicular amplitudes of vibration (*K*), harmonic vibrational corrections ($\alpha/2$) to the observed rotation constants (B_0), and corrections to bond lengths upon isotopic substitution were then calculated from the scaled force constants using ASYM40.

Structural Analysis

Microwave Spectroscopy. Difluoromaleic anhydride shows a rich *b*-type asymmetric-rotor spectrum ($\kappa = +0.08$) with many vibrational satellites. Both the ground- and excited-state spectral intensities show the 3:1 nuclear spin statistical weightings associated with the exchange of two equivalent fluorine atoms ($I = {}^1/_2$). Taken together with the ground-state inertial defect values ($\Delta = I_c - I_a - I_b$) for the main species, $\Delta = 0.0202(2)$ u $Å^2$, and the isotopic species, these observed spin statistics establish unequivocally the molecule to be planar with C_{2v}

TABLE 1: Nozzle-to-Plate Distances, Weighting Functions, Correlation Parameters, Scale Factors, and Electron Wavelengths for the Combined GED/MW Study

nozzle-to-plate distance, mm	Δs[a]	s_{min}[a]	sw_1[a]	sw_2[a]	s_{max}[a]	correlation parameter	scale factor k[b]	electron wavelength,[c] pm
285.94	2	20	40	122	144	0.490	0.804(8)	5.672
128.22	4	60	80	304	356	0.453	0.667(11)	5.675

[a] In nm^{-1}. [b] Figures in parentheses are the estimated standard deviations (1σ). [c] Determined by reference to the scattering pattern of benzene.

symmetry. The inertial defect is accounted for satisfactorily by the harmonic force-field calculations. The ring structure can be calculated directly by isotopic substitution and the C−F bonds placed from the moment equations. The fluorine coordinates were derived using the first- and second-moment equations for the substitution structure, but the second-moment equations were preferred for the r_z structure. Planar moments were used in Kraitchman's equations[26] for both the substitution and average structures. In adopting isotopic shrinkage corrections in the calculation of the r_z parameters, it was necessary to estimate changes in ring angles commensurate with bond length changes derived from ASYM40. Table 6 gives the r_s (substitution) and r_z structures calculated from the experimental microwave data.

The permanent dipole moment lies along the C_2 symmetry axis (Figure 1) such that $\mu_{total} = \mu_b$, and $\mu_a = \mu_c = 0$. The dipole moment has been determined from high-resolution Stark measurements on several transitions for the vibrational ground-state including the $J = 6 \leftarrow 5$ as detailed in Table 7. In deriving the experimental second-order Stark coefficients, it was necessary to make corrections for fourth-order effects. The experimental dipole moment of 1.867(3) D obtained for DFMA agrees well with the vector sum (1.76 D) of maleic anhydride (3.95 D),[8] and the C−F bond moment obtained from *cis*-1,2 difluoroethene ($\mu_{total} = 2.43$ D).[27]

Figure 2 shows a typical transition from the spectrum in which the ground-state line is clearly accompanied by two vibrational series. The series to low-frequency belongs to a vibration with torsional (a_2) symmetry at 154(10) cm^{-1}, with the same spin statistics as the ground state, and the other to an out-of-plane ring-bending (b_1) vibration at 102(12) cm^{-1} showing 1:3 alternation. The wavenumber values have been determined by relative intensity measurements averaged over 10 and 5 transitions for the torsional and bending modes, respectively. These values correspond to those of maleic anhydride at 266(20) and 168(15) cm^{-1}, respectively.[28] Table 8 gives the rotation constants and inertial defects of these modes in difluoromaleic anhydride versus vibrational quantum number. The values for the inertial defects agree well with the values (cm^{-1}) determined from relative intensity measurements, the large negative values being typical of low-frequency out-of-plane modes.

Electron Diffraction. Assuming that difluoromaleic anhydride has C_{2v} symmetry, eight independent parameters are required to define the structure. As the radial-distribution curve (Figure 3) contains only five distinct peaks, it was expected that strong correlation between parameters would make it difficult to refine all of the geometrical parameters simultaneously; in particular, the C═C and C−F bond lengths would be very similar to one another. The independent parameters (Table 9) needed to represent the five different bonded distances were chosen to be their weighted mean (p_1), the difference between the mean of r(C−C) and r(O−C) and the weighted mean of the C═C, C−F, and C═O bond lengths (p_2), the difference between r(C−C) and r(O−C) (p_3), the difference between the weighted mean of the C−F and C═C bond lengths and r(C═O) (p_4), and the difference between r(C═C) and r(C−F) (p_5). The other three parameters were defined to be the internal ring angle C═C−C (p_6), and the external ring angles C═C−F (p_7) and C−C═O (p_8).

The radial-distribution curve (Figure 3) shows all the interatomic bonded distances lying under the broad peak centered at ca. 135 pm, with the two-bond nonbonded distances associated uniquely with the feature at ca. 220 pm. The three-bond O···F and F···F distances account for the peak near 300 pm, the remaining three-bond nonbonded distances all lying under the peak at ca. 350 pm. The two four-bond distances lie under the feature at $r > 400$ pm, the O···O distance represented by a shoulder at ca. 450 pm.

Two $r_\alpha°$ refinements of the structure were undertaken, one using the ED data alone (ED), while in the latter the ED data and the rotation constants (B_z) were fitted simultaneously (ED/MW). Starting values for the refinements were taken from the theoretical geometry and vibrational force-field computations at the MP2/6-31G(d) level. The results are compared in Table 9.

Using the ED data alone, it was possible to refine simultaneously seven of the eight independent geometrical parameters. Allowing p_5, the difference between the C═C and C−F bond lengths, to refine freely returned a value of 4.8(19) pm, the large uncertainty reflecting the high degree of correlation between it and other refining parameters. Consequently, the C═C bond distance, at 135.3(16) pm, was poorly defined and appeared unreasonably long compared to the value determined experimentally from the MW data [$r_z = 132.5(4)$ pm)] and predicted ab initio [$r_e = 133.6$ pm at MP2/6-311+G(2df)]. Since fixing the value of p_5 in the final refinement undoubtedly leads to an underestimate of the errors for other refining parameters with which it is correlated, it was refined using a flexible restraint.[29]

Flexible restraints may allow the refinement of parameters which would otherwise have to be fixed.[29] Estimates of the values of these restrained quantities and their uncertainties are used as additional observations in a combined analysis similar to those routinely carried out for electron-diffraction data combined with rotation constants and/or dipolar coupling constants.[12] The values and uncertainties for the extra observations are derived from another method such as X-ray diffraction or theoretical computations. *All* geometrical parameters are then included in the refinements. In cases where a restrained parameter is also a refinable parameter, if the intensity pattern contains useful information concerning the parameter, it will refine with an esd less than the uncertainty in the corresponding additional observation. However, if there is essentially no relevant information, the parameter will refine with an esd approximately equal to the uncertainty of the extra observation and its refined value will equal that of the restraint. In this case, if the correlation matrix also shows no correlation with other refining parameters, the parameter can simply be fixed, in the knowledge that doing this does not influence either the magnitudes or the esd's of other parameters. In some cases, because increasing the number of refining parameters allows all effects of correlation to be considered, some esd's may increase. Overall, this approach utilizes all available data as fully as possible and returns more realistic esd's for refining

TABLE 2: Measured and Calculated[a] Ground-State Rotational Transition Frequencies (MHz)

(a) Normal Species

J'	K_a'	K_c'	J''	K_a''	K_c''	ν_{obs}	$\nu_{(obs-calc)}$	J'	K_a'	K_c'	J''	K_a''	K_c''	ν_{obs}	$\nu_{(obs-calc)}$
2	2	1	1	1	0	8147.351[b]	0.006	10	1	9	9	2	8	23203.75	0.03
2	2	0	1	1	1	9267.348[b]	0.000	10	2	9	9	1	8	23204.29	0.01
4	4	1	3	3	0	18011.69	−0.08	10	7	3	9	6	4	41534.53	−0.07
4	0	4	3	1	3	9034.503[b]	−0.001	10	3	8	9	2	7	25250.57	0.09
4	1	4	3	0	3	9129.894[b]	0.003	10	1,0	10	9	0,1	9	21182.78	0.06
5	5	1	4	4	0	22836.57	−0.06								
5	5	0	4	4	1	22890.82	−0.06	10	2	8	9	3	7	25230.23	0.07
5	1	5	4	0	4	11108.959[b]	−0.001	10	3	7	9	4	6	27151.42	0.13
5	0	5	4	1	4	11086.593[b]	−0.001	10	4	7	9	3	6	27512.73	0.03
6	5	1	5	4	2	25964.14	0.07	11	8	3	11	7	4	11916.73	−0.14
6	5	2	5	4	1	25516.30	−0.09	11	1	11	10	0	10	23199.98	−0.03
6	4	3	5	1	4	31964.78	−0.10	11	3	8	10	4	7	29264.29	0.04
6	4	3	5	3	2	22235.92	−0.13	11	4	7	10	5	6	30871.97	0.05
6	6	0	5	5	1	27631.44	−0.01	11	5	7	10	4	6	32106.68	0.17
6	6	1	5	5	0	27616.80	−0.05	11	1	10	10	2	9	25220.36	0.01
6	5	2	5	4	1	25516.30	−0.09	11	6	6	10	5	5	36689.80	0.11
7	6	1	6	5	2	30583.92	−0.08	11	2	10	10	1	9	25220.48	0.02
7	2	5	6	3	4	18806.99	−0.12	11	3	9	10	2	8	27253.97	0.06
7	5	2	6	4	3	29524.71	0.00	11	0	11	10	1	10	23199.98	−0.03
7	5	3	6	4	2	27682.37	−0.10	12	0,1	12	11,0	1	11	25217.31	−0.01
7	7	0	6	6	1	32385.55	−0.13								
7	7	1	6	6	0	32381.94	−0.05	12	1,2	11	11	2,1	10	27237.13	0.04
8	4	5	7	3	4	24623.92	0.04								
8	8	1	7	7	0	37142.67	−0.04	13	6	7	13	5	8	11949.57	−0.06
8	5	3	7	4	4	34072.46	−0.04	13	5	9	13	4	10	18418.13	−0.13
8	6	2	7	5	3	33744.36	−0.08	13	4	9	13	3	10	18390.34	−0.06
8	5	4	7	4	3	29162.71	−0.02	13	0,1	13	12	1,0	12	27234.63	−0.01
8	7	2	8	6	3	11650.35	−0.03								
8	7	2	7	6	1	35252.19	−0.05	13	2	12	12	1	11	29254.01	0.03
9	2	7	8	3	6	23193.74	0.04	13	8	5	13	7	6	9021.830	0.00
9	3	6	9	2	7	12340.18	0.11	13	1	12	12	2	11	29254.01	0.03
9	5	5	8	4	4	30136.20	0.08	14	4	10	14	3	11	20469.88	0.00
9	1	8	8	2	7	21186.74	−0.03	14	1	13	14	0	14	27124.03	0.12
9	2	8	8	1	7	21189.40	−0.03	14	0	14	13	1	13	29251.94	−0.03
9	3	6	8	4	5	24824.53	0.01	14	2	13	14	1	14	27124.03	0.12
9	4	6	8	3	5	25892.66	0.08	14	2,3	12	13	3,2	11	33294.98	0.05
9	6	4	8	5	3	34862.19	0.01								
9	6	3	8	5	4	37504.73	−0.07	14	1	14	13	0	13	29251.94	−0.02
9	3	7	8	2	6	23273.34	0.09	14	6	9	13	5	8	39801.09	−0.03
9	9	0	8	8	1	41902.41	0.04	15	5	10	14	6	9	41437.89	−0.07
9	9	1	8	8	0	41902.21	0.05	15	9	6	15	8	7	9915.610	0.16
10	5	6	9	4	5	30980.09	0.08	23	15	8	23	14	9	22825.71	0.06
10	7	4	10	6	5	11453.09	0.04								
10	6	5	9	5	4	36020.98	−0.15								

(b) Isotopic Species

						$^{18}O_6$		$^{18}O_1$	
J'	K_a'	K_c'	J''	K_a''	K_c''	ν_{obs}	$\nu_{(obs-calc)}$	ν_{obs}	$\nu_{(obs-calc)}$
6	5	2	5	4	1	25180.81	0.10		
6	6	1	5	5	0			27045.87	0.02
7	6	1	6	5	2			30038.76	0.03
7	6	2	6	5	1	30017.93	0.07		
7	7	1	6	6	0	31992.03	−0.02	31709.12	0.03
7	7	0	6	6	1	31994.54	0.01	31714.28	−0.03
8	7	2	7	6	1	34769.86	−0.10	34572.15	−0.03
8	7	1	7	6	2	34800.64	−0.06		
8	8	1	7	7	0			36366.81	−0.02
9	2	8	8	1	7	20671.70	−0.01		
10	1,0	10	9	0,1	9	20663.46	0.08	20985.47	0.07
10	3	8	9	2	7	24642.19	0.08	25007.71	0.03
10	5	6	9	4	5	30668.56	0.01	30313.31	0.01
11	0,1	11	10	1,0	10	22631.15	−0.04		
11	1	10	10	2	9	24602.42	−0.01	24984.97	−0.03
11	2	10	10	1	9	24602.64	−0.01	24985.03	−0.02
11	3	8	10	4	7	28526.70	0.02	29001.68	0.07
11	4	7	10	5	6	29873.75	−0.01	30748.13	−0.02
11	5	7	10	4	6	31622.18	0.01		
12	0,1	12	11	1,0	11	24598.99	−0.04	24982.44	0.00
12	1,2	11	11	2,1	10	26569.68	0.03	26982.97	−0.07
13	0,1	13	12	1,0	12	26566.86	−0.02	26980.97	−0.01

						$^{13}C_2$[b]		$^{13}C_3$[b]	
J'	K_a'	K_c'	J''	K_a''	K_c''	ν_{obs}	$\nu_{(obs-calc)}$	ν_{obs}	$\nu_{(obs-calc)}$
4	1	4	3	0	3	9098.080	0.000		
4	0	4	3	1	3	9001.161	0.001	9019.020	0.000
5	0	5	4	1	4	11046.516	0.001	11067.358	0.000
5	1	5	4	0	4	11069.382	−0.001	11089.520	0.000

[a] Derived rotational constants (B) are given in Table 3 (Fitted in the III^{r}representation). [b] Fourier-transform measurements.

TABLE 3: Ground-State Spectroscopic Constants[a] from the MW Study (*B*/MHz, Δ/u Å²)

	isotopomer/substitution				
constant	[1] parent	[2] $^{13}C_2$	[3] $^{13}C_3$	[4] $^{18}O_6$	[5] $^{18}O_1$
A_0[b]	2379.5563(6)	2373.688(9)	2374.628(6)	2353.3685(16)	2327.7705(14)
B_0[b]	1750.9848(8)	1743.248(4)	1748.339(2)	1691.0397(30)	1751.0467(36)
C_0[b]	1008.6812(2)	1005.0585(8)	1006.9260(4)	983.9487(6)	999.2885(7)
A_z	2379.1129	2373.247	2374.193	2352.936	2327.350
B_z	1751.0408	1743.303	1748.399	1691.086	1751.113
C_z	1008.6228	1005.002	1006.8681	983.8921	999.2310
Δ_0	0.0202(2)	0.0201(11)	0.0160(4)	0.0193(10)	0.0149(5)
Δ_z	0.0188	0.0188	0.0158	0.0175	0.0157

[a] Figures in parentheses are the estimated standard deviations (1σ). [b] Conversion factor of 505379.1 MHz u Å².

TABLE 4: Theoretical (r_e) Geometrical Parameters (distances/pm, angles/deg)[a]

	level of theory/basis set					
parameter	SCF/6-31G(d)	MP2/6-31G(d)	SCF/6-311G(d)	MP2/6-311G(d)	MP2/6-311G(2df)	MP2/6-311+G(2df)
$r(C_2{=}O_6)$	116.8	120.3	116.1	119.3	119.1	119.2
$r(C_3{-}F_8)$	129.6	132.4	129.1	131.3	130.6	130.6
$r(C_3{=}C_4)$	131.2	134.1	131.0	134.0	133.6	133.6
$r(O_1{-}C_2)$	136.0	140.0	135.7	139.1	138.8	138.9
$r(C_2{-}C_3)$	148.8	148.5	148.8	149.9	148.2	148.2
$\angle C_2C_3{=}C_4$	108.1	108.4	108.0	108.1	108.1	108.2
$\angle C_4{=}C_3F_8$	130.7	130.3	130.7	130.6	130.4	130.1
$\angle C_3C_2{=}O_6$	129.0	129.2	128.8	128.8	128.9	129.1
$\angle C_2O_1C_5$	110.5	108.8	110.4	108.8	108.8	108.9
$\angle O_1C_2C_3$	106.7	107.2	106.8	107.5	107.5	107.4

[a] For atom-numbering scheme, see Figure 1.

TABLE 5: Observed (anharmonic) and Calculated (harmonic) Fundamental Vibrational Frequencies (cm^{-1})

		theoretical[a]		
symmetry	mode	unscaled	scaled[b]	expt[c]
a_1	ν_1	1914	1881	1885 (IR)
	ν_2	1821	1765	1763 (IR)
	ν_3	1330	1297	1280 (IR)
	ν_4	1156	1131	1141 (IR)
	ν_5	678	671	676 (IR)
	ν_6	624	630	630 (R)
	ν_7	377	382	385 (R)
	ν_8	248	258	257 (R)
a_2	ν_9	656	683	not observed
	ν_{10}	470	490	not observed
	ν_{11}	110	115	[154 (MW)][d]
b_1	ν_{12}	706	735	735 (IR)
	ν_{13}	312	325	325 (R)
	ν_{14}	159	166	[102 (MW)][d]
b_2	ν_{15}	1860	1823	1820 (IR)
	ν_{16}	1438	1404	1392 (IR)
	ν_{17}	1088	1057	1062 (IR)
	ν_{18}	948	934	933 (IR)
	ν_{19}	733	761	756 (R)
	ν_{20}	517	525	523 (R)
	ν_{21}	297	303	305 (R)
rms % error (excluding a_2 modes and ν_{14})		2.7	0.6	

[a] Calculated at the MP2/6-31G(d) level. [b] Details of scaling are given in the Supporting Information. [c] Key: IR = infrared of gas; R = Raman of liquid; MW = microwave. [d] Frequency not included when scaling force constants.

parameters; the unknown effects of correlation with otherwise fixed parameters are revealed and included.[30]

For p_5, a restraint of 2.3 pm with an uncertainty of ±0.7 pm was employed, these values being derived from the results of the ab initio computations reported in Table 5. Subsequently, p_5 refined to 2.6(6) pm with all other parameters returning realistic values and esd's. In particular, the esd for the C=C bond length increased by a factor of 2.5, i.e., $r(C{=}C)$ = 133.6(5) pm compared to 133.3(2) pm when p_5 was fixed.

All amplitudes of vibration pertaining to nonbonded distances could be refined freely. However, it was necessary to apply restraints to the ratios of refining amplitudes tied together in pairs. The values of these ratio restraints were taken from the scaled MP2/6-31G(d) force field with uncertainties of 2.5% of the absolute values. Attempts to refine the amplitudes for the five bonded distances using a similar approach were unsuccessful. Instead $u(C{-}F)$ and the four ratios of $u(C{-}F)$ with the other amplitudes for bonded distances were restrained. For the final cycle, R_G = 0.0903 (R_D = 0.0503).

In the combined ED/MW refinements, 15 rotation constants determined from the microwave spectra of five different isotopomers, viz. the parent [1] ($^{12}C_{2-5}$, $^{16}O_{1,6,7}$, $^{19}F_{8,9}$) with

TABLE 6: Geometrical Parameters Refined from the MW Data (distances/pm, angles/deg)[a]

	structure type	
parameter	r_s	r_z[b]
$r(C_2{=}O_6)$	119.2	118.3(4)
$r(C_3{-}F_8)$	132.1	131.3(4)
$r(C_3{=}C_4)$	131.8	132.5(4)
$r(O_1{-}C_2)$	139.3	139.7(2)
$r(C_2{-}C_3)$	147.5	148.7(6)
$\angle C_2C_3{=}C_4$	108.64	108.65(1)
$\angle C_4{=}C_3F_8$	130.27	130.09(9)
$\angle C_3C_2{=}O_6$	129.93	129.92(1)
$\angle C_2O_1C_5$	108.47	109.09(31)
$\angle O_1C_2C_3$	107.13	106.81(16)

[a] For atom-numbering scheme, see Figure 1. [b] Estimated errors (1σ) in parentheses calculated as absolute $^1/_2(r_z - r_s)$.

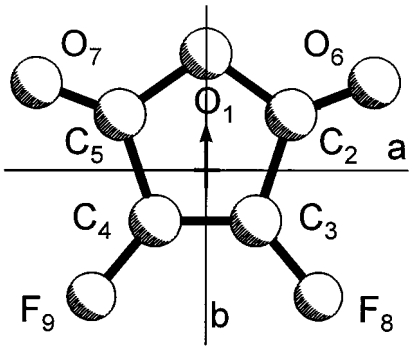

Figure 1. Molecular structure of difluoromaleic anhydride as refined from the ED/MW study. Principal rotation axes (a and b) and the direction of the dipole moment are shown.

TABLE 7: Stark Measurements and Dipole Moment[a]

								$\Delta\nu_{corr}{}^b/E^2$ (MHz kV^{-2} cm^{-2})	
J'	K_a'	K_c'		J''	K_a''	K_c''	M	expt	calcd
6	5	2	←	5	4	1	2	−14.059(44)	−14.052
6	5	2	←	5	4	1	3	−34.959(44)	−35.001
6	4	3	←	5	3	2	2	−23.092(83)	−23.123

$\mu_b = \mu_{total} = 1.8665(33)$ D

[a] Figures in parentheses are the standard deviations (1σ); calibration μ(OCS) = 0.7152(2) D; 1D = 3.33564×10^{-30} C m. [b] $\Delta\nu_{corr} = \Delta\nu$ corrected for fourth-order effects.

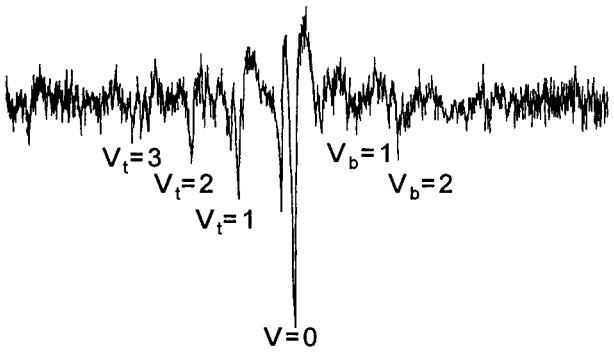

Figure 2. Part of the microwave spectrum recorded between 9.6 and 10.1 GHz using a 1000 Vcm^{-1} Stark field. This is the $15_{96} \leftarrow 15_{87}$ transition showing vibrational satellites associated with the low-frequency torsional mode (V_t) and the out-of-plane bending mode (V_b).

substitution $^{13}C_2$ [2], $^{13}C_3$ [3], $^{18}O_6$ [4], and $^{18}O_1$ [5], were combined with the GED data. The corrected rotational data B_z were presented in the refinements as the three absolute values for the parent isotopomer, A[1], B[1], and C[1], and the differences of the other isotopomers for each axis from these values, i.e., A[1] − A[2], B[1] − B[2], C[1] − C[2], etc. (Table 10).

The vibrational corrections to the microwave constants ($B_0 \rightarrow B_z$) for each isotopomer are summations of the corrections for each mode.[25] These sums were small, ca. 0.44 MHz for the *A* axis and ca. 0.06 MHz for the *B* and *C* axes, but contributions from some individual modes were of the order of 5 MHz. The 10% error in the absolute value of the vibrational correction normally assumed was deemed inappropriately small. Instead, the uncertainty in the absolute correction was computed from a summation of an assumed 10% error in the correction for each mode, according to eq 1 below, where $c(m)_i$ is the vibrational correction of the *i*th mode of the main isotopomer, i.e., A[1], B[1], or C[1]. The uncertainty in the correction for a difference between the rotation constants for two isotopomers was calculated similarly, as in eq 2, where $c(n)_i$ is the vibrational correction of the *i*th mode of isotopomer *n*, i.e., A[1] − A[*n*], B[1] − B[*n*], and C[1] − C[*n*], ($n = 2-5$).

$$\sqrt{\sum_i \left[\frac{c(m)_i}{10}\right]^2} \quad (1)$$

$$\sqrt{\sum_i \left[\frac{c(m)_i - c(n)_i}{10}\right]^2} \quad (2)$$

Simultaneous refinement of the ED and MW data permitted p_5 to be refined freely. The data from the two methods demonstrated a good degree of compatibility, with 11 of the 15 rotation constants fitting within the estimated uncertainties of the corrected experimental values (see Table 10). Of the other four, only the calculated value for A[1] − A[4] lay outwith 2× the uncertainty range, corresponding to B_z(obs − calc) = 0.06 MHz. Although such slight incompatibilities may be assigned to small changes in the ring angles on isotopic substitution which are not allowed for in our model, the scatter of differences is consistent with the expected pattern for the quoted uncertainties. Relative to the ED-only refinement, there was a slight increase (0.001) in R_G accompanied by a significant reduction in the estimated uncertainties of all geometrical parameters.

The success of the final ED/MW refinement, for which R_G = 0.091 (R_D = 0.059), may be assessed on the basis of the difference between the experimental and calculated radial-distribution curves (Figure 3). The interatomic distances and vibrational amplitudes (and restraints) of the optimum refinement are listed in Table 11. The least-squares correlation matrix is given as part of the Supporting Information together with the experimental molecular-scattering intensity curves.

Discussion

The experimental measurements described herein provide the first structural information for 3,4-difluorofuran-2,5-dione. The analyses of both the microwave (Table 6) and the electron-diffraction (Table 9) data are consistent with the spectroscopic evidence that the molecule consists of a planar five-membered ring incorporating a C═C double bond with C_{2v} symmetry in the gas phase. Studies of the structure in the solid phase by single-crystal X-ray crystallography (not detailed here) have been frustrated to date by the growth of crystals of inadequate quality for high-resolution measurements. However, preliminary data suggest strongly that the structure in the solid phase is also molecular with C_{2v}, or near C_{2v}, symmetry.[31]

The geometrical parameters refined experimentally from the microwave data alone and from the combined microwave/electron-diffraction data agree well (Table 12); at the 3σ (99.7% probability) level, the only significant differences lie with the angles $C_2C_3{=}C_4$ [MW: 108.65(1)°; GED/MW: 108.3(1)°] and $C_3C_2{=}O_6$ [MW: 129.92(1)°; GED/MW: 129.3(1)°]. In the GED/MW combined analysis, all correlation between refining parameters is included in the error estimates by the use of flexible restraints. There are effectively no systematic errors in the electron wavelength and camera distances since the data for the benzene calibrant are treated identically to that of the compound. Systematic errors must result from not allowing for changes in bond angles on isotopic substitution and from excluding the two lowest-frequency modes from the vibrational analysis (underestimation of *K* corrections). However, it is not possible to say which esd's are affected explicitly and, moreover, ignoring such deficiencies is not expected to give rise to significantly underestimated errors. We therefore quote the estimated standard deviations, 1σ, with the proviso that one or two parameters may be defined slightly less precisely than this would indicate.

The structural parameters predicted at the MP2 level of theory are in very good quantitative agreement with those obtained experimentally (Tables 4 and 12). From the graded series of ab initio calculations detailed in Table 4, it is clear that an account of the correlated motion of electrons is essential if such good quantitative agreement between theory and experiment is to be obtained. The inclusion of electron correlation at the MP2 level leads to a marked increase in all bond lengths of double-bond character and of bonds to the highly electronegative O and F atoms, relative to the uncorrelated SCF computations, e.g., SCF/6-31G(d) vs MP2/6-31G(d); this is as expected for electron precise molecules.[32] Optimum agreement with experimental

TABLE 8: Excited-State Spectroscopic Constants[a] from the MW Study (*B*/MHz, Δ/(u Å²), *D*,*d*,*σ*/kHz)

constant	$V = 0$	1 (bend)	2 (bend)	1 (torsion)	2 (torsion)
A	2379.5563(6)	2375.506(6)	2371.470(3)	2373.743(1)	2368.138(4)
B	1750.9847(8)	1752.458(4)	1753.913(2)	1747.332(4)	1743.882(4)
C	1008.6812(2)	1009.613(4)	1010.586(4)	1007.187(4)	1005.878(22)
D_J	0.1706(50)	ω(bend) = 102(12) cm^{-1}		ω(torsion) = 154(10) cm^{-1}	
D_{JK}	−0.2814(60)				
D_K	0.11176[b]				
$d1$	−0.0416(46)				
$d2$	−0.0272(33)				
σ	6				
n	84				
Δ[c]	0.0202(2)	−0.562(2)	−1.167(2)	−0.361(2)	−0.783(11)

[a] Figures in parentheses are the estimated standard deviations (1σ). [b] Fixed at MP2/6-31G(d) force-field value. [c] $\Delta = I_c - I_b - I_a$, conversion factor of 505379.1 MHz u Å^2.

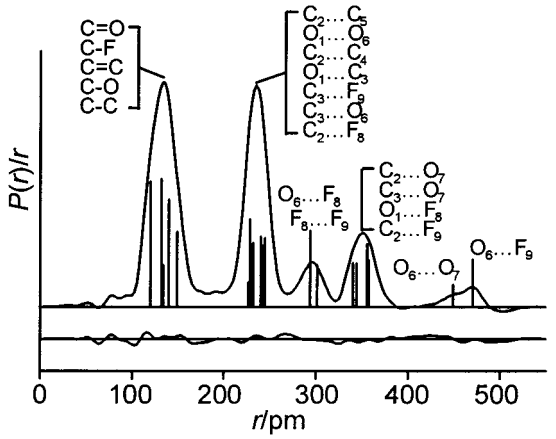

Figure 3. Observed and final weighted difference radial-distribution curves. Before Fourier inversion the data were multiplied by s exp[(−0.000 02s^2)/($Z_C - f_C$)($Z_F - f_F$)].

TABLE 9: Geometrical Parameters (r_α°/$\angle_\alpha$) for the Electron-Diffraction Study (r/pm, angle/deg)[a,b]

no.	parameter	ED[c]	ED/MW[c]
	(a) Independent		
p_1	1/9[2r(O_1−C_2) + 2r(C_2−C_3) + 2r(C_3−F_8) + r(C_3=C_4) + 2r(C_2=O_6)]	134.3(1)	134.29(1)
p_2	1/2[r(C_2−C_3) + r(O_1−C_2)] − 1/5[2r(C_3−F_8) + r(C_3=C_4) + 2r(C_2=O_6)]	17.6(4)	17.3(2)
p_3	r(C_2−C_3) − r(O_1−C_2)	9.9(6)	9.2(3)
p_4	1/3[2r(C_3−F_8) + r(C_3=C_4)] − r(C_2=O_6)	13.3(4)	12.7(1)
p_5	r(C_3=C_4) − r(C_3−F_8)	2.6(6)	2.3(4)
p_6	∠C_2C_3=C_4	108.0(2)	108.3(1)
p_7	∠C_4=C_3F_8	130.0(11)	129.9(1)
p_8	∠C_3C_2=O_6	128.2(5)	129.3(1)
	(b) Dependent		
d_1	r(C_2=O_6)	118.5(3)	119.0(1)
d_2	r(C_3−F_8)	130.9(3)	130.9(2)
d_3	r(C_3=C_4)	133.6(5)	133.2(3)
d_4	r(O_1−C_2)	139.1(4)	139.3(1)
d_5	r(C_2−C_3)	149.0(3)	148.5(2)
d_6	∠$C_2O_1C_5$	108.3(7)	108.9(1)
d_7	∠$O_1C_2C_3$	107.9(5)	107.2(1)

[a] For atom-numbering scheme, see Figure 1. [b] Figures in parentheses are the estimated standard deviations (1σ). [c] For details of the refinements, see the text.

parameters is found when the basis set is extended to triple-ζ quality including additional d- and f-type polarization functions, as has been observed elsewhere for wave functions which account for electron correlation.[32] Diffuse functions were not found to offer any significant improvement. Thus, at the MP2 level with the 6-311G(2df) basis set, theoretical parameters offer excellent support for those derived experimentally.[33]

TABLE 10: Microwave Rotation Constants (*B*/MHz) Used in the GED Refinements

constant[a]	B_Z(obs)[b]	B_Z(calc)[c]	B_Z(obs − calc)	uncertainty[d]
A[1]	2379.1125	2379.8913	−0.7788	1.0058
B[1]	1751.0413	1750.5843	0.4570	0.4476
C[1]	1008.6231	1008.6491	−0.0260	0.1087
A[1] − A[2]	5.866	5.858	0.008	0.018
B[1] − B[2]	7.738	7.742	−0.004	0.121
C[1] − C[2]	3.6226	3.6232	−0.0006	0.0052
A[1] − A[3]	4.920	4.916	0.004	0.020
B[1] − B[3]	2.642	2.630	0.012	0.053
C[1] − C[3]	1.7550	1.7564	−0.0014	0.0054
A[1] − A[4]	26.1767	26.1178	0.0589	0.0181
B[1] − B[4]	59.9549	59.9469	0.0080	0.0631
C[1] − C[4]	24.7309	24.7289	0.0020	0.0072
A[1] − A[5]	51.7628	51.7006	0.0552	0.0400
B[1] − B[5]	−0.0720	0.0001	−0.0721	0.0969
C[1] − C[5]	9.3921	9.4057	−0.0136	0.0083

[a] Isotopomer numbering: [1] = parent (^{12}C, ^{16}O, ^{19}F); [2] = $^{13}C_2$; [3] = $^{13}C_3$; [4] = $^{18}O_6$; [5] = $^{18}O_1$. [b] From microwave spectroscopy. $B_0 \rightarrow B_Z$ corrections were derived from the MP2/6-31G(d) force field using ASYM40. [c] From the GED/MW refinement. [d] For details of the derivation of uncertainty estimates, see the text.

TABLE 11: Interatomic Distances and Amplitudes of Vibration for the Combined GED/MW Study (r_a, u/pm)[a,b]

no.	atom pair	distance (r_a)	amplitude (u)	restraint
r_1	C_2=O_6	119.6(1)	3.6(1)	$u_2 = 4.2 \pm 0.1$
r_2	C_3−F_8	131.4(2)	4.1(1)	$u_2/u_1 = 1.149 \pm 0.029$
r_3	C_3=C_4	133.6(3)	3.9(1)	$u_2/u_3 = 1.017 \pm 0.025$
r_4	O_1−C_2	139.6(1)	4.9(2)	$u_2/u_4 = 0.841 \pm 0.021$
r_5	C_2−C_3	148.7(3)	4.8(1)	$u_2/u_5 = 0.855 \pm 0.021$
r_6	C_2···C_5	226.7(2)	5.6(2)	$u_7/u_6 = 1.022 \pm 0.026$
r_7	O_1···O_6	228.3(2)	5.7(2)	$u_7/u_8 = 1.048 \pm 0.026$
r_8	C_2···C_4	228.6(2)	5.4(2)	$u_7/u_9 = 1.015 \pm 0.025$
r_9	O_1···C_3	232.0(2)	5.6(2)	
r_{10}	C_3···F_9	239.7(2)	5.1(2)	$u_{10}/u_{11} = 0.975 \pm 0.024$
r_{11}	C_3···O_6	242.6(1)	5.2(3)	$u_{10}/u_{12} = 0.874 \pm 0.022$
r_{12}	C_2···F_8	244.5(1)	5.9(3)	
r_{13}	O_6···F_8	293.7(2)	10.8(5)	$u_{13}/u_{14} = 1.006 \pm 0.025$
r_{14}	F_8···F_9	301.3(2)	10.8(5)	
r_{15}	C_2···O_7	340.5(2)	8.7(4)	$u_{15}/u_{16} = 1.029 \pm 0.026$
r_{16}	C_3···O_7	344.1(2)	8.5(4)	
r_{17}	O_1···F_8	355.9(1)	9.8(4)	$u_{17}/u_{18} = 1.041 \pm 0.026$
r_{18}	C_2···F_9	357.6(1)	9.4(4)	
r_{19}	O_6···O_7	448.9(2)	10.4(7)	
r_{20}	O_6···F_9	470.2(1)	10.5(7)	$u_{20}/u_{19} = 1.015 \pm 0.025$

[a] For atom-numbering scheme, see Figure 1. [b] Figures in parentheses are the estimated standard deviations (1σ).

The observed experimental vibrational frequencies for liquid-phase (Raman) and vapor-phase (IR) samples of difluoromaleic anhydride are listed as part of the Supporting Information. Harmonic frequencies calculated at the MP2/6-31G(d) level are given in Table 5. An assignment of the experimental fundamental frequencies has been made (Table 5), on the basis of a

TABLE 12: Geometrical Parameters of 3,4-Disubstituted Maleic Anhydrides (distances/pm, angles/deg)[a,b]

	H			F			Cl		Br
parameter	MW (r_s)	GED (r_a)	ab initio (r_e)[c]	MW (r_z)	GED/MW ($r_\alpha°$)	ab initio (r_e)[c]	GED (r_a)	ab initio (r_e)[c]	ab initio (r_e)[c]
$r(C_2{=}O_6)$	119.62(1)	119.5(3)	120.6	118.3(4)	119.0(1)	120.3	118.8(2)	120.3	120.3
$r(C_3\text{-}X_8)$	107.91(3)	109.1(21)	108.3	131.3(4)	130.9(2)	132.4	168.5(2)	168.9	184.7
$r(C_3{=}C_4)$	133.31(4)	133.0(30)	134.0	132.5(4)	133.2(3)	134.1	133.2(5)	134.8	134.7
$r(O_1{-}C_2)$	138.76(1)	139.4(11)	139.9	139.7(2)	139.3(1)	140.0	138.9(3)	139.7	139.9
$r(C_2{-}C_3)$	148.49(3)	150.0(5)	148.8	148.7(6)	148.5(2)	148.5	149.5(3)	149.2	149.1
r_{ring}(mean)[d]	141.56(6)	142.4(35)	142.3	141.9(10)	141.8(4)	142.2	142.0(8)	142.5	142.5
$\angle C_2C_3{=}C_4$	107.90(1)	107.7(10)	108.2	108.65(1)	108.3(1)	108.4	107.9(2)	108.1	108.2
$\angle C_4{=}C_3X_8$	129.99(0)	128.9(33)	129.5	130.09(9)	129.9(1)	130.3	129.4(4)	129.8	129.2
$\angle C_3C_2{=}O_6$	129.61(1)	129.3(20)	129.7	129.92(1)	129.3(1)	129.2	128.5(4)	129.4	129.6
$\angle C_2O_1C_5$	108.06(1)	107.0(11)	108.3	109.09(31)	108.9(1)	108.8	108.2(6)	109.0	109.1
$\angle O_1C_2C_3$	108.07(0)	108.8(12)	107.7	106.81(16)	107.2(2)	107.2	108.1(4)	107.4	107.3
$\Delta\angle_{int.\ ring}$[e]	0.17(1)	1.8(16)	0.6	2.3(4)	1.7(1)	1.6	0.3(6)	1.6	1.8
ref	8	7	this work	this work	this work	this work	10	this work	this work

[a] For atom-numbering scheme, see Figure 1. [b] Estimated errors given in parentheses are as quoted in the original work. [c] MP2/6−31(d) level. [d] $r_{ring}(\text{mean}) = 1/5[r(C_3{=}C_4) + 2\,r(O_1{-}C_2) + 2\,r(C_2{-}C_3)]$. [e] Maximum difference of internal ring angles.

careful comparison of both the experimental and theoretical frequencies and their intensities.[34] In general, the theoretical values are found to differ by no more than 4% of the assigned experimental frequency. The exceptions are the two lowest-frequency modes, ν_{11} and ν_{14}, corresponding to a ring torsional (a_2) mode and an out-of-plane ring bending (b_1) mode, which have not been observed directly. From the MP2/6-31G(d) level force field (scaled or unscaled), the a_2 mode is predicted to lie at lower frequency than the b_1 mode, $\Delta\nu = (\nu_{14} - \nu_{11}) = 49$ cm^{-1}. However, microwave vibrational satellite intensities (Figure 2) show that the b_1 mode has the lowest fundamental frequency in the molecule, $\Delta\nu = -52(16)$ cm^{-1}. Unfortunately, support for the MW measurements was not available from the experimental vibrational spectra since (i) there are a number of features in the Raman spectrum of the liquid below 200 cm^{-1}, so unambiguous assignment of two frequencies to the a_2 and b_1 modes is not possible, and (ii) facilities were not available to record far-infrared spectra which potentially would identify the b_1 mode, the a_2 being inactive. However, the microwave frequencies are consistent with those of maleic anhydride itself, at 168(15) cm^{-1} (b_1) and 266(20) cm^{-1} (a_2), i.e., $\Delta\nu = -98$-(25) cm^{-1},[28] both being ca. 0.6 of the analogous mode in the parent anhydride (0.58 for the torsion and 0.61 for the bend), suggesting a similar change in reduced mass for the two modes on substituting H for F. Thus, it would appear that these modes are incorrectly ordered in the ab initio computations and were subsequently excluded from the force-field analysis. This notwithstanding, inclusion of such low-frequency modes is known to result in an overestimation of perpendicular amplitudes of vibration (K).[34]

For vibrational frequencies in multiply bonded species, it is not uncommon to find the greatest discrepancies between the experimental and theoretical frequencies for low-magnitude bending and torsional modes.[35] It is more uncommon to find the theoretical calculation opposing the relative magnitudes of these experimental frequencies. However, force-field computations for difluoromaleic anhydride at a higher level, or employing a DFT approach, yielded almost identical predictions for $\Delta\nu$, viz., 47 cm^{-1} at MP2/6-311G(d) and 46 cm^{-1} at B3LYP/6-31G(d), cf. 49 cm^{-1} at MP2/6-31G(d). Further, calculations for the maleic anhydride and for dichloro- and dibromomaleic anhydrides were also undertaken. For each, the relative ordering of the lowest-frequency modes, even at the uncorrelated SCF/6-31G(d) level, is in accord with the experimental observations.[36,37] This suggests that the discrepancy between theory and experiment for such modes in the present case must arise as a result of the presence of fluorine in the molecule.

Although all of the 3,4-dihalofuran-2,5-diones are known, only the structure of the dichloro derivative has been reported (a gas-phase electron-diffraction study),[10] together with the structure of the parent maleic anhydride in the solid phase by X-ray crystallography[38] and as a vapor by microwave spectroscopy[8] and electron diffraction.[7] The results of these studies are collected together in Table 12. Bearing in mind that the data refer to definitions of experimental parameters that differ slightly, viz., r_s (MW) vs r_a (GED) and $r_\alpha°$ (GED) $\equiv r_z$ (MW), and that the errors for the GED determination of maleic anhydride are relatively large,[7] the studies to date suggest strongly that a change in substituent leads to very little change in the structure. Thus, the three structures investigated experimentally demonstrate the same average ring size to within experimental error [see r_{ring}(mean)], and show very little ring distortion relative to a regular pentagon (108°), as judged by the range of the internal ring angles.

To support our experimental findings, further ab initio computations have been undertaken to optimize the structures of maleic anhydride and its 3,4-dichloro and 3,4-dibromo derivatives. At the MP2/6-31G(d) level, the agreement between the parameters for which experimental data are available is good, and allows the relative magnitudes of the theoretical values to be compared with confidence.

The average ring size for the Cl and Br derivatives is predicted to be slightly larger than for X = H or F, attributable mainly to the longer $C_2{-}C_3$ single-bond distances in the heavier congenors, but the variation falls over only 0.3 pm. The predicted distortion of the ring shows a systematic increase, the trend in internal ring-angle difference being H < F = Cl < Br, but, as found experimentally, the variation is very small [(0.6°(H) − 1.8°(Br)].

For the 3,4-disubstituted maleic anhydrides considered here (X = H, F, Cl, or Br), there is a significant variation in the size of the substituent atom, Br ≈ Cl > F > H, and in its electronegativity, F > Cl ≈ Br > H.[11] These variations give rise to structural changes which originate from four steric/electronic effects. First, increasing the steric demands of the substituent would lead primarily to a wider C=C−X angle and, consequently, to a wider C−C=O angle. A second, similar distortion would be expected on increasing the electronegativity of the substituent atom as a result of greater electrostatic repulsion of the pairs C−X/C−X and C−X/C=O. From the ab initio values in Table 12, it is seen that neither trend is borne out, in that for angle C=C−X the ordering is F > Cl > H > Br and for ∠C−C=O it is H > Br > Cl > F, the latter demonstrating the reverse trend from that expected of the

SCHEME 2

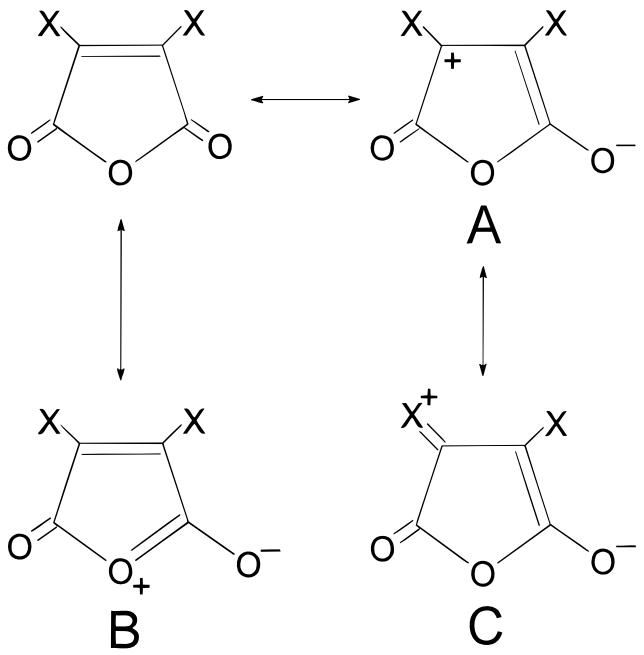

electronegativity. Another effect associated with an increase in substituent electronegativity is well-known; namely, that bonds adjacent to C−X are expected to become shorter [*r*(C═C) and *r*(C−C)] and the internal (ipso) angle (∠C═C−C) to widen.[39] At the vicinal, carbonyl position *r*(C═O) and *r*(C−O) would be expected to shorten to a lesser degree and the angles C−C−O and C−C═O to narrow. The calculations predict H < F < Cl < Br, F < H < Cl < Br for *r*(C═C) and *r*(C−C) and Cl < Br = H < F for ∠C═C−C. For *r*(C═O) and *r*(C−O) the ordering is F = Cl = Br < H and Cl < Br = H < F, and F < Br < Cl < H and F < Cl < Br < H for ∠C−C−O and ∠C−C═O, respectively. Thus, only the angles at the vicinal carbon follow the trend anticipated from this third effect which is observed widely in aromatic systems.[40] However, for X = F the average ring size would be expected to be smallest, and this appears to be borne out by the MP2/6-31G* computations (Table 12), albeit marginally. Finally, the structural implications of charge delocalization must be considered, for which the canonical forms, **A**, **B**, and **C**, in Scheme 2 are illustrative. Form **B**, representing delocalization across O═C−O−C═O, makes an essentially equivalent contribution to each of the disubstituted anhydrides. Form **A** involves the localization of positive charge adjacent to the substituent and is thus disfavored with increasing electronegativity of X. It would lead to longer *r*(C═C) and *r*(C═O) bond lengths, a shorter *r*(C−C) bond, a wider C−C═O angle, and a narrower C−C−X angle. The expected trend is followed only for the C−C═O angle, for which H > Br > Cl > F, while *r*(C═O) is longest for X = H, although equal for all others. This is not surprising since the trend for the stabilization of form **C** is opposite to that of form **A**; form **C** involves a π-type donation from *X* to the positively charged carbon center and is favored particularly for X = F (≫ Cl > Br) but not observed for X = H. It is an analogue of form **C** which accounts for fluorobenzene having the smallest dipole moment of the halobenzenes. Ultimately, therefore, it is the interplay of these four steric and electronic effects, none of which appears to dominate, that gives rise to the great similarity between the structures of maleic anhydride and its 3,4-dihalo derivatives.

Acknowledgment. We are indebted to the Engineering and Physical Sciences Research Council (EPSRC) for support of the Edinburgh Electron-Diffraction Service (Grant GR/K44411) and the Edinburgh ab initio facilities (Grant GR/K04194), and to Rhône-Poulenc Chemicals (Avonmouth) for financial support (O.J.D.). We thank Professor A. C. Legon (University of Exeter) for obtaining the FTMW spectra and Mr. S. Hawker (University of Bristol) for assistance with analysis, Dr. T. M. Greene (University of Oxford) and Dr. C. R. Pulham (University of Edinburgh) for collecting the FT Raman spectra, and Dr. L. Hedberg (Oregon State University) for providing a copy of the ASYM40 program.

Supporting Information Available: Consisting of five tables, listing (i) observed vibrational frequencies, (ii) internal and symmetry coordinates, (iii) scale and quadratic force constants, (iv) significant (≥ 50) elements of the correlation matrix, and (v) Cartesian coordinates for the experimental (ED/MW) and theoretical structures, and a plot of the molecular-scattering intensity curves. This material is available free of charge via the Internet at http://pubs.acs.org.

References and Notes

(1) Abdo, B. T.; Banks, R. E. Unpublished work.
(2) Abdo, B. T.; Banks, R. E. *J. Fluorine Chem.* **1992**, *58*, 360.
(3) Raasch, M. S.; Miegel, R. E.; Castle, J. E. *J. Am. Chem. Soc.* **1959**, *81*, 2678.
(4) Ciamician, A.; Silber, P. *Chem. Ber.* **1883**, *16*, 2396.
(5) Ciamician, A. *Chem. Ber.* **1891**, *24*, 1347.
(6) Diels, O.; Reinback, M. *Chem. Ber.* **1910**, *43*, 1273.
(7) Hilderbrandt, R. L.; Peixoto, E. M. A. *J. Mol. Struct.* **1972**, *12*, 31.
(8) Stiefvater, O. L. *Z. Naturforsch* **1978**, *33A*, 1480.
(9) A citation search of the Beilstein Database for 3,4-disubstituted furan-2,5-diones yields 800 (H), 8 (F), 72 (Cl), 18 (Br), and 5 (I).
(10) Hagen, K.; Hedberg, K. *J. Mol. Struct.* **1978**, *50*, 103.
(11) For example, see: Emsley, J. *The Elements*; Clarendon Press: Oxford, 1989.
(12) Abdo, B. T.; Alberts, I. L.; Attfield, C. J.; Banks, R. E.; Blake, A. J.; Brain, P. T.; Cox, A. P.; Pulham, C. R.; Rankin, D. W. H.; Robertson, H. E.; Murtagh, V.; Heppeler, A.; Morrison, C. *J. Am. Chem. Soc.* **1996**, *118*, 209.
(13) Brisdon, A.; Brain, P. T.; Bühl, M.; Robertson, H. E.; Rankin, D. W. H. Unpublished results.
(14) Kobrina, L. S.; Akulenko, N. V.; Yakobson, G. G. *Zh. Org. Khim.* 1972, **8**, 2165.
(15) Huntley, C. M.; Laurenson, G. S.; Rankin, D. W. H. *J. Chem. Soc., Dalton Trans.* **1980**, 954.
(16) Cradock, S.; Koprowski, J.; Rankin, D. W. H. *J. Mol. Struct.* **1981**, *77*, 113.
(17) Brain, P. T.; Mitzel, N. W.; Rankin D. W. H. *ED96 Program*, updated from Boyd, A. S. F.; Laurenson, G. S.; Rankin, D. W. H. *J. Mol. Struct.* **1981**, *71*, 217.
(18) Ross, A. W.; Fink, M.; Hilderbrandt, R. *International Tables for Crystallography*; Wilson, A. J. C., Ed.; Kluwer Academic Publishers: Dordrecht, The Netherlands, Boston, MA, London, 1992; Vol. C, p 245.
(19) Frisch, M. J.; Trucks, G. W.; Schlegel, H. B.; Gill, P. M. W.; Johnson, B. G.; Robb, M. A.; Cheesman, J. R.; Keith, T. A.; Petersson, G. A.; Montgomery, J. A.; Raghavachari, K.; Al-Laham, M. A.; Zakrzewski, V. G.; Ortiz, J. V.; Foresman, J. B.; Cioslowski, J.; Stefanov, B. B.; Nanayakkara, A.; Challacombe, M.; Peng, C. Y.; Ayala, P. Y.; Chen, W.; Wong, M. W.; Andres, J. L.; Replogle, E. S.; Gomperts, R.; Martin, R. L.; Fox, D. J.; Binkley, J. S.; Defrees, D. J.; Baker, J.; Stewart, J. P.; Head-Gordon, M.; Gonzalez, C.; Pople, J. A. *Gaussian 94*, revision C2; Gaussian Inc.: Pittsburgh, PA, 1995.
(20) Hehre, W. J.; Ditchfield, R.; Pople, J. A. *J. Chem. Phys.* **1972**, *56*, 2257.
(21) Hariharan, P. C.; Pople, J. A. *Theor. Chim. Acta* **1973**, *28*, 213.
(22) Gordon, M. S. *Chem. Phys. Lett.* **1980**, *76*, 163.
(23) Krishnan, R.; Binkley, J. S.; Seeger, R.; Pople, J. A. *J. Chem. Phys.* **1980**, *72*, 650.
(24) McLean, A. D.; Chandler, G. S. *J. Chem. Phys.* **1980**, *72*, 5639.
(25) Hedberg, L.; Mills, I. M. *J. Mol. Spectrosc.* **1993**, *160*, 117.
(26) Kraitchman, J. *Am. J. Phys.* **1953**, *21*, 17.
(27) Laurie, V. W. *J. Chem. Phys.* **1961**, *34*, 291.
(28) Caminati, W.; Giorgini, M. G.; Ruiz-Pastrana, M.; Alonso, J. L. *Spectrochim. Acta* **1985**, *41A*, 937.
(29) Blake, A. J.; Brain, P. T.; McNab, H.; Miller, J.; Morrison, C. A.; Parsons, S.; Rankin, D. W. H.; Robertson, H. E.; Smart, B. A. *J. Phys.*

Chem. **1996**, *100*, 12280. (b) Brain, P. T.; Morrison, C. A.; Parsons, S.; Rankin, D. W. H. *J. Chem. Soc., Dalton Trans*. **1996**, 4589.

(30) Brain, P. T.; Bühl, M.; Robertson, H. E.; Jackson, A. D.; Lickiss, P. D.; MacKerracher, D.; Rankin, D. W. H.; Shah, D.; Thiel, W. *J. Chem. Soc., Dalton Trans*. **1998**, 545, and references therein.

(31) Amer, H.; Banks, R. E.; Brain, P. T.; Murtagh, V.; Rankin, D. W. H.; Parsons, S. Unpublished results.

(32) Hehre, W.; Radom, L.; Schleyer, P. v. R.; Pople, J. A. *Ab Initio Molecular Orbital Theory*; Wiley: New York, 1986.

(33) It should be borne in mind, however, that this procedure involves comparison of two different structure types, viz., ground-state average r_α° (from GED) and r_e (from theory) geometries. For example, see: Hargittai, I.; Hargittai, M. *Molecular Structures and Energetics, Vol. II, Physical Measurements*; VCH: New York, 1988; Chapter 20, p 417.

(34) For example, see: Ma, B.; Lii, J.-H.; Chen, K.; Allinger, A. L. *J. Am. Chem. Soc*. **1997**, *119*, 2570, and references therein.

(35) This procedure involves comparison of two different types of vibrational frequencies, namely fundamental (from IR and Raman spectroscopy) and harmonic (from theory). For example, see (a) Simandiras, E. D.; Handy, N. C.; Amos, R. D. *J. Phys. Chem*. **1988**, *92*, 1739. (b) Simandiras, E. D.; Rice, J. E.; Lee, T. J.; Amos, R. D.; Handy, N. C. *J. Chem. Phys*. **1988**, *88*, 3187.

(36) (a) Rogstad, A.; Klaboe, P.; Baranska, H.; Bjarnov, E.; Christensen, D. H.; Nicolaisen, F.; Nielsen, O. F.; Cyvin, B. N.; Cyvin, S. J. *J. Mol. Struct*. **1974**, *20*, 403. (b) Le Gall, L.; Caillet, P.; Forel, M.-T. *J. Chim. Phys*. **1978**, *75*, 444.

(37) (a) Rogstad, A.; Klaboe, P.; Cyvin, B. N.; Cyvin, S. J.; Christensen, D. H. *Spectrochim. Acta* **1972**, *28A*, 111. (b) Ishibashi, Y.; Shimada, R.; Shimada, H. *Bull. Chem. Soc. Jpn*. **1983**, *56*, 1362.

(38) Marsh, R. E.; Ubell, E.; Wilcox, H. E. *Acta Cryst*. **1962**, *15*, 35.

(39) (a) Gillespie, R. J. *J. Chem. Educ*. **1970**, *47*, 18, (b) Gillespie, R. J. *Molecular Geometry*; Van Nostrand Reingold: New York, 1972.

(40) For example, see: Hargittai, I.; Hargittai, M. *Molecular Structures and Energetics, Vol. II, Physical Measurements*; VCH: New York, 1988; Chapter 7, p 281.

(41) *Handbook of Chemical Physics*; Lide, D. R., Frederiske, H. P. R., Eds.; CRC: London, 1993; Chapter 9, p50.